



## Effect of Negatively Charged Ions on the Formation of Microarc Oxidation Coating on 2024 Aluminium Alloy

Wei Yang<sup>1)</sup>, Bailing Jiang<sup>2)</sup>, Aiyang Wang<sup>1)†</sup> and Huiying Shi<sup>2)</sup>

1) Ningbo Key Laboratory of Marine Protection Materials, Ningbo Institute of Materials Technology and Engineering, Chinese Academy of Sciences, Ningbo 315201, China

2) School of Materials Science and Engineering, Xi'an University of Technology, Xi'an 710048, China

[Manuscript received May 31, 2011, in revised form December 2, 2011]

The present study deals with the effect of negatively charged ions on the ceramic coating formation on 2024 aluminium alloy during microarc oxidation (MAO) process. On the basis of the experimental results, two steps (the formation of an incipient film without arc presence and the growth of a ceramic coating with arc discharge) of MAO process have been observed. For comparison, four different negatively charged ions studied. It is proved that negatively charged ions strongly participated in the formation of an incipient film with high impedance value at the first step. The growth of ceramic coating depends on the combination between Al of the substrate and O from the electrolyte, and the negatively charged ions are little consumed. As an anodic oxide coating is prepared on the sample surface instead of the incipient film, the first step occurs easily and the growth of ceramic coating is accelerated. Furthermore, the mechanism of negatively charged ions in the formation of the MAO coating has been proposed.

**KEY WORDS:** Aluminium alloy; Microarc oxidation; Incipient film; Ceramic coating; Negatively charged ions

### 1. Introduction

Microarc oxidation (MAO, also named as plasma electrolytic oxidation or anodic spark oxidation) is a simple and clean technique to fabricate ceramic coatings on the light alloy surface utilizing microarc discharge generated by dielectric breakdown<sup>[1,2]</sup>. The performance of light alloy is enhanced largely, such as wear, friction, corrosion resistance<sup>[3–7]</sup>, which extends the applications of light alloy<sup>[8–10]</sup>. Through the observation of experimental phenomenon, it is proved that the formation of MAO coating can be divided into two stages<sup>[11]</sup>, the formation of an incipient film without arc presence and the growth of a ceramic coating with arc discharge. Although several investigations have been carried out so far, such as the character and formation of the MAO coating<sup>[12–16]</sup>, the mechanism of negatively charged ions in the formation of ceramic coating has not been well understood.

Up to now, it has been found that the arc discharge phenomenon is obviously different in the electrolytes with different negatively charged ions addition. In the practical application, it is hoped that the arc striking phenomenon can easily occur by means of understanding the function of negatively charged ions during the MAO process.

In this study, the aluminium substrate was treated by MAO equipment in the four different solutions. The surface features of the films formed at two different steps in the four different electrolytes were investigated. Finally, the mechanism of negatively charged ions in the formation of the MAO coating was proposed.

### 2. Experimental

A 2024 aluminium alloy having the nominal composition Cu3.8%–4.9%, Mg1.2%–1.8%, Mn0.3%–0.9%, Ti≤0.15%, Zn≤0.3%, Fe≤0.5%, Si≤0.5%, Ni≤0.15% was used as the substrate in the present study. The samples of Ø20 mm×5 mm were fabricated. The electrolytes containing different negatively charged ions

† Corresponding author. Prof., Ph.D.; Tel.: +86 574 86685036; Fax: +86 574 86685159; E-mail address: aywang@nimte.ac.cn (A.Y. Wang).

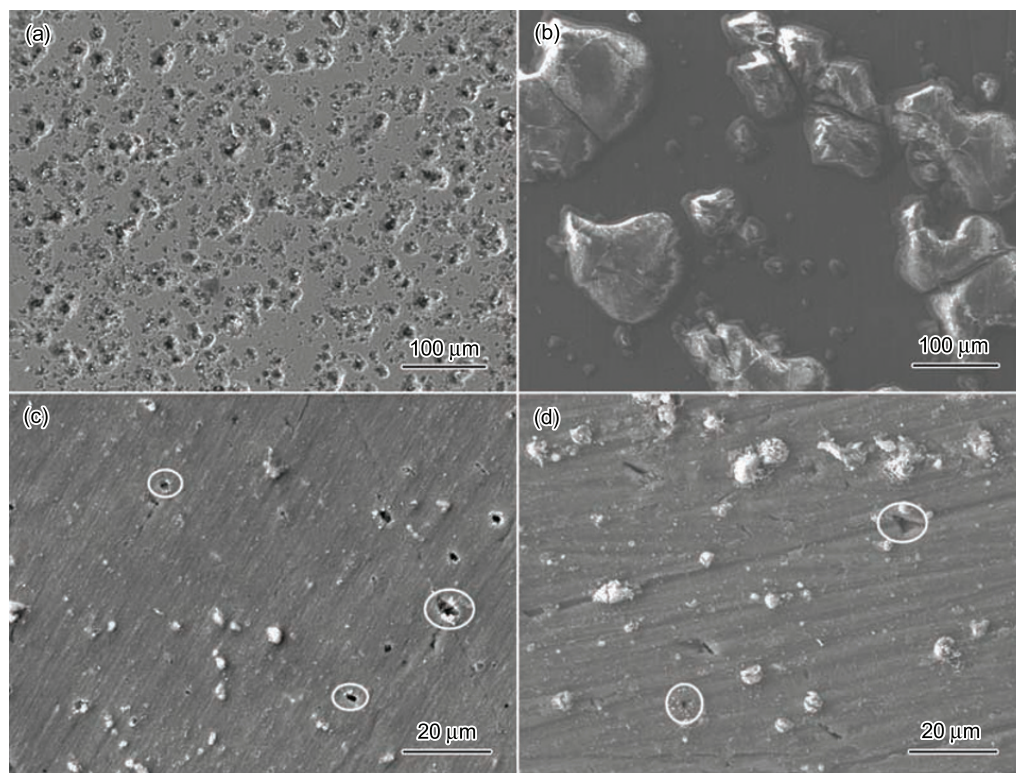


**Fig. 1** Surface morphologies of incipient films in the four electrolytes: (a) 0.1 mol/L NaCl; (b) 0.1 mol/L Na<sub>2</sub>SO<sub>4</sub>; (c) 0.1 mol/L Na<sub>2</sub>SiO<sub>3</sub>; (d) 0.1 mol/L Na<sub>2</sub>CO<sub>3</sub>

(Cl<sup>-</sup>, SO<sub>4</sub><sup>2-</sup>, SiO<sub>3</sub><sup>2-</sup> and CO<sub>3</sub><sup>2-</sup>, 0.1 mol/L respectively) were used in the experiment. The ceramic coatings were fabricated with an alternating-current MAO system. The service consisted of a potential adjustable AC power supply up to 750 V, a stirring system and cooling system, *etc.* The temperature of the electrolyte was controlled below 30 °C and the applied current density, pulse frequency, duty ratio, duration time was fixed at 5 A/dm<sup>2</sup>, 400 Hz, 10% and 8 min, respectively. A prefab coating was prepared on the sample surface by anodic oxidation under 100 V for 10 min in the oxalic acid (38 g/L) aqueous solution at 21 °C. The different thickness or impedance values of prefab coatings were obtained by controlling the oxidation time and voltage.

The surface morphology of the coating was examined by using a JEOL jsm-6700F scanning electron microscope (SEM). The impedance value of the incipient film was measured by using IM6e electrochemical workstation. Electrochemical experiments were conducted in 5% NaCl solution. A Pt and a saturated calomel electrode were used as counter and reference electrodes, respectively. Electrochemical impedance spectroscopy (EIS) spectra was acquired at the open circuit potential in the frequency range 10<sup>6</sup>–10<sup>-2</sup> Hz. X-Ray diffraction (XRD) analysis was performed to identify the different phases of the coatings. The chemical states of Si and C contained in the MAO coatings were investigated by X-ray photoelectron spectroscopy (XPS).

### 3. Results and Discussion

#### 3.1 SEM and XPS analysis of incipient film

Fig. 1 illustrates the surface features of the incipient films formed in the four electrolytes. It can be obtained that a large number of corrosion regions distribute on the sample surface formed in the NaCl solution (Fig. 1(a)), and the impedance value of this film is 482 Ω. The film surface formed in the Na<sub>2</sub>SO<sub>4</sub> solution shows a concavo-convex surface feature (Fig. 1(b)), and its impedance value is 568 Ω. In the above two electrolytes, the arc striking phenomenon is not observed. Fig. 1(c)–(d) show the presence of several discharge channels on the incipient film surface formed in the Na<sub>2</sub>SiO<sub>3</sub> and Na<sub>2</sub>CO<sub>3</sub> solutions, and the impedance values of the films are 36005 Ω and 22670 Ω, respectively. In the above two solutions, the arc discharge is discovered. So it is believed that the formation of a compact coating with high impedance value on the sample surface is a primary condition for the arc striking.

The chemical state of Si or C on the incipient film surface is investigated by XPS. XPS survey spectra and high-resolution spectra are shown in Fig. 2(a)–(d), respectively. The Si2p peaks of 103.05 eV and 101.59 eV of the incipient coating formed in the Na<sub>2</sub>SiO<sub>3</sub> solution indicate the existence of Al<sub>2</sub>SiO<sub>5</sub> and SiO<sub>x</sub>. The C1s peak of 282.35 eV of the incipient coating formed in the Na<sub>2</sub>CO<sub>3</sub> solution indicates

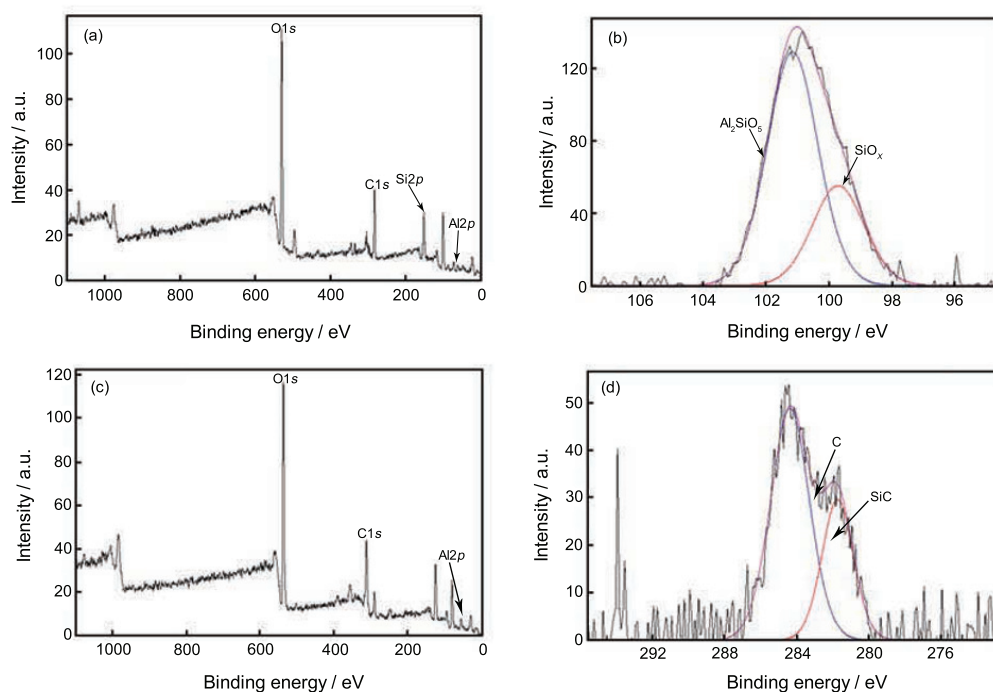


**Fig. 2** XPS survey spectra (a) from the incipient film surface formed by MAO in  $\text{Na}_2\text{SiO}_3$  electrolyte and high-resolution spectra (b) at the  $\text{Si}2p$  region, (c) from the film surface formed by MAO in  $\text{Na}_2\text{CO}_3$  electrolyte and high-resolution spectra (d) at the  $\text{C}1s$  region

the existence of  $\text{SiC}$ , which may be the scrap during the sample preparation. So it is proposed that the element of  $\text{Si}$  from the negatively charged film strongly participated in forming the incipient film.

### 3.2 SEM and XPS analysis of ceramic coating

Fig. 3 illustrates the surface features of the coatings formed by MAO for 8 min in the four electrolytes. As shown in Fig. 3(a), the corrosion region also appears on the sample surface in the  $\text{NaCl}$  solution, which gets worse compared with the incipient film. Fig. 3(b) illustrates that some volcano-like bulges with a size around  $5\text{--}10\ \mu\text{m}$  in diameter appear on the sample surface in the  $\text{Na}_2\text{SO}_4$  solution, which still does not have a ceramic character. As shown in Fig. 3(c) and (d), the surface feature of the ceramic coating formed in the  $\text{Na}_2\text{SiO}_3$  or  $\text{Na}_2\text{CO}_3$  solution is porous, and the micropore diameters are range from 1 to  $5\ \mu\text{m}$ .

The chemical state of  $\text{Si}$  or  $\text{C}$  on the ceramic coating surface was further investigated using XPS. XPS survey spectra and high-resolution spectra are shown in Fig. 4(a)–(d). The weak  $\text{Si}2p$  peak of  $103.05\ \text{eV}$  of the ceramic coating formed in the  $\text{Na}_2\text{SiO}_3$  solution indicates the existence of  $\text{Al}_2\text{SiO}_5$ , and the peak of  $\text{SiO}_x$  disappears compared with the incipient film. In the  $\text{Na}_2\text{CO}_3$  solution, the weak  $\text{C}1s$  peak of  $\text{SiC}$  does not exist on the ceramic coating surface. So it is believed that the element of  $\text{C}$  did not participate in the growth of ceramic coating.

### 3.3 Growth characteristics of coated sample with a prefab coating

In view of the above, it is proved that the formation of a compact coating with high impedance value on the sample surface is a primary condition for the arc striking. So it is essential in detail to investigate the effect of prefab coating with high impedance values on the formation of MAO coatings.

The varieties of arc striking time and voltage of the coated sample in the  $\text{Na}_2\text{SiO}_3$  solution are shown in Tables 1 and 2, respectively. The coatings with the different impedance values at the similar thickness or with the different thickness at the similar impedance value are formed by anodic oxidation. It can be seen that the arc striking time and voltage of the coated sample are independent of the impedance value and thickness of the prefab coating. So it is believed that if only a prefab coating was prepared on the sample surface, it will be helpful for occurring arc striking phenomenon.

Fig. 5 shows the variations of voltage as a function of oxidation time during MAO process in the four electrolytes. As shown in Fig. 5 (a), the voltage rapidly increases in the first 1 min and then tends to be stable in the  $\text{NaCl}$  solution. As an anodic oxide coating is prepared on the sample surface, the stable voltage obviously increases and arc striking phenomenon still does not occur. As shown in Fig. 5(b), the stable voltage is  $280\ \text{V}$  and the arc striking phenomenon does

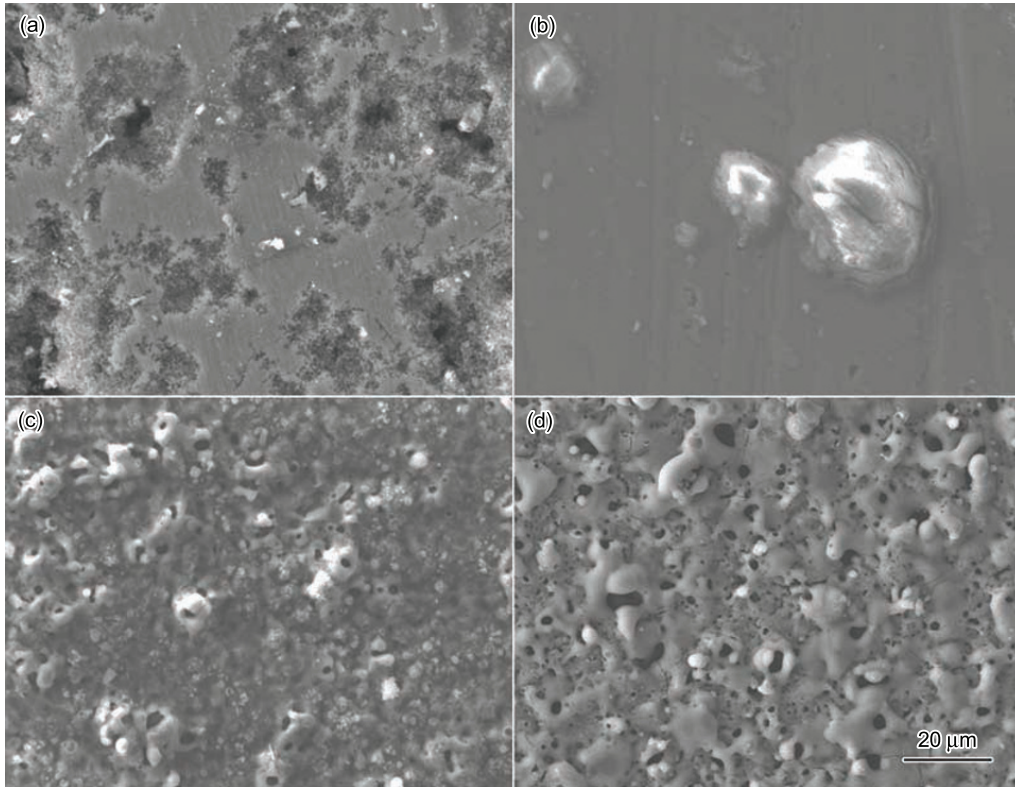


**Fig. 3** Surface morphologies of the coatings formed in the four electrolytes: (a) 0.1 mol/L NaCl; (b) 0.1 mol/L Na<sub>2</sub>SO<sub>4</sub>; (c) 0.1 mol/L Na<sub>2</sub>SiO<sub>3</sub>; (d) 0.1 mol/L Na<sub>2</sub>CO<sub>3</sub>

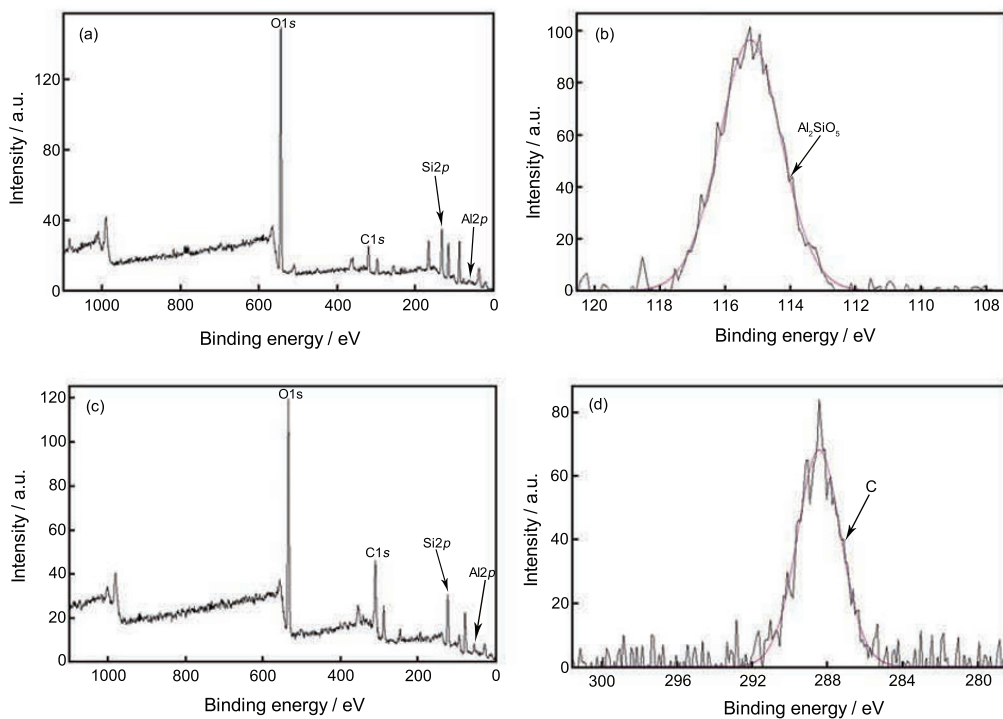


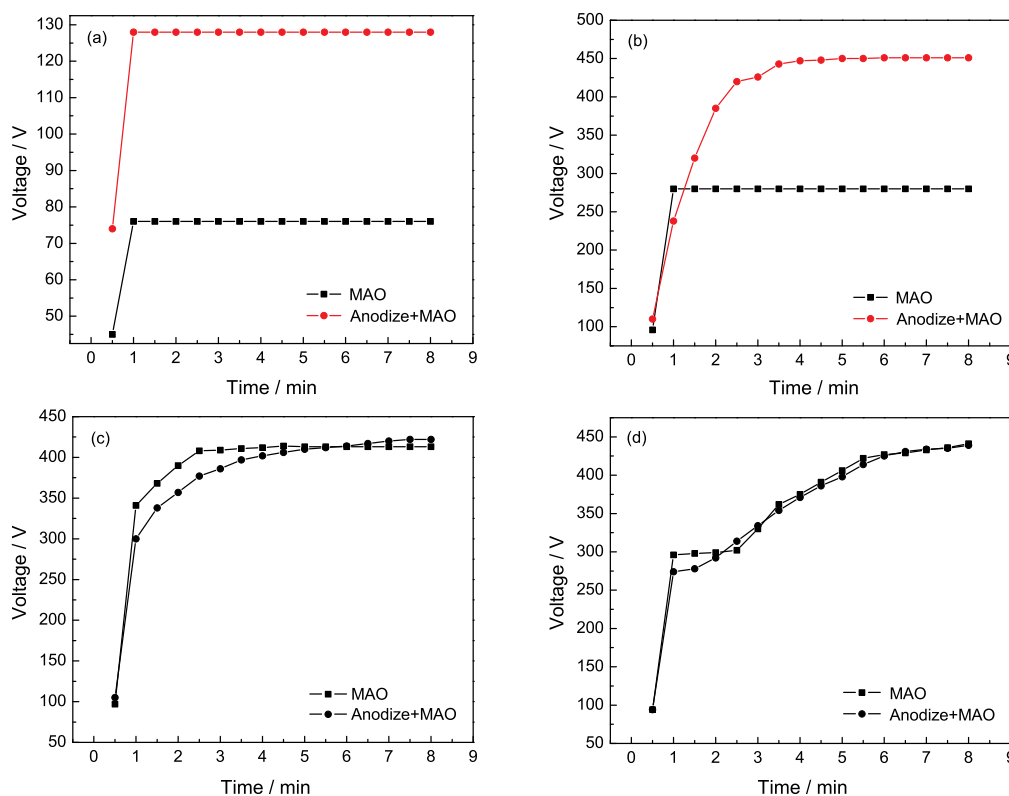
**Fig. 4** XPS survey spectra (a) from the ceramic coating surface formed by MAO in Na<sub>2</sub>SiO<sub>3</sub> electrolyte for 8 min and high-resolution spectra (b) at the Si2p region, (c) from the ceramic coating surface formed by MAO in Na<sub>2</sub>CO<sub>3</sub> electrolyte for 8 min and high-resolution spectra (d) at the C1s region

**Table 1** Arc striking time and voltage of the coated sample with different thickness

Thickness/ $\mu\text{m}$	Arc striking voltage/V	Arc striking time/s
8	243	41
16.2	242	41
28.1	262	43

**Table 2** Arc striking time and voltage of the coated sample with different impedance values

Impedance value/ $\Omega$	Arc striking voltage/V	Arc striking time/s
482	222	39
1003	232	41
11413	229	40

**Fig. 5** Dependence of voltage on oxidation time in different electrolytes: (a) 0.1 mol/L NaCl; (b) 0.1 mol/L  $\text{Na}_2\text{SO}_4$ ; (c) 0.1 mol/L  $\text{Na}_2\text{CO}_3$ ; (d) 0.1 mol/L  $\text{Na}_2\text{SiO}_3$ 

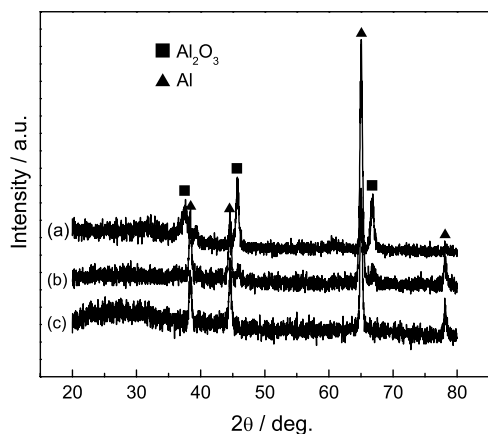
not occur in the  $\text{Na}_2\text{SO}_4$  solution. As a prefab coating is prepared on the sample surface, the stable voltage can reach 450 V and the arc striking phenomenon occurs. Fig. 5(c) and (d) show that whether a prefab coating is prepared on the sample surface, the arc striking phenomenon occurs easily and the growth curves of ceramic coating have a similar change in the  $\text{Na}_2\text{SiO}_3$  or  $\text{Na}_2\text{CO}_3$  solution.

Fig. 6 illustrates XRD spectra of the coatings prepared by the different techniques. It is found that the diffraction peak of the Al substrate is strong and the alumina phase is not discovered on the anodic oxide coating. The characteristic diffraction peaks of alumina formed by MAO on the coated sample surface are strong compared with the sample without a prefab coating. It is known that the conventional anodic oxide coating is a very thin alumina film, possibly existing as amorphous or not fully crystalline alumina.

### 3.4 Discussion

In the above experiment, the variations of arc striking phenomenon and growth curves are shown in the solution with addition of different negatively charged ions. Furthermore, the compositions of the incipient film and ceramic coating formed at the two stages are also compared. As different anodic oxide coatings are prepared on the sample surface, the arc striking phenomenon and growth curves during MAO process are all similar.

It is known that negatively charged ions will move towards the sample surface by means of the electromigration. As a result, an electric double layer is formed at the substrate-solution interface, and the electric field intensity can reach  $10^9$  V/cm. Negatively charged ions with different chemical characters will be selected into this electric field, which may



**Fig. 6** XRD spectra of the coatings formed by different techniques: (a) anodic oxidation 10 min+MAO 30 min; (b) MAO 30 min; (c) anodic oxidation 10 min

result in the growing difference.

The arc discharge occurs on the sample surface as an active electrode after the formation of incipient film, which is prior to the negatively charged ions in the electrolytes. Then a large number of  $\text{Al}^{3+}$  is generated on the sample surface. In the  $\text{NaCl}$  or  $\text{Na}_2\text{SO}_4$  solution, a deposition layer with high impedance value can not be formed on the sample surface for their dissolution characteristics of  $\text{Cl}^-$  or  $\text{SO}_4^{2-}$ , and also the insulation of anodic electrode is not increased effectively. As a result, the arc striking phenomenon does not occur. In the  $\text{Na}_2\text{SiO}_3$  or  $\text{Na}_2\text{CO}_3$  solution,  $\text{SiO}_3^{2-}$  or  $\text{CO}_3^{2-}$  is easily combined with  $\text{Al}^{3+}$  to form an insulation layer with high impedance value, which results in the increase of voltage with the oxidation time, and certainly the arc striking phenomenon occurs.

The arc discharge of Al substrate is restricted by the negatively charged ions after the formation of incipient film with high impedance value on the sample surface. It is known that the discharge order is  $\text{Cl}^- > \text{OH}^- > \text{oxy salt}$ . So it can be seen that a large number of gas appears on the sample surface in the  $\text{NaCl}$  solution, and the arc striking phenomenon cannot occur in this electrolyte. In the  $\text{Na}_2\text{SiO}_3$  or  $\text{Na}_2\text{CO}_3$  solution,  $\text{OH}^-$  as the hydrolysate of negatively charged ions is abundant in the electrolyte. So a great deal of oxygen is generated under this strong electric field, and the chemical reaction of oxygen and aluminium is processed by the instantaneously high temperature in the heat-affected zone<sup>[17,18]</sup>. Meanwhile the momentary concentration of  $\text{H}^+$  on the sample surface increases quickly due to the arc discharge of  $\text{OH}^-$ , which results in the ceramic coating dissolved. So another function of the negatively charged ions such as  $\text{SiO}_3^{2-}$  and  $\text{CO}_3^{2-}$  is to combine with  $\text{H}^+$  and restrain the dissolution of ceramic coating. It can be seen that the arc striking phenomenon can not occur in the  $\text{Na}_2\text{SO}_4$  solution, which may attribute to its dissolution function. As an anodic oxide coating is prepared on the sample surface, arc striking phenomenon occurs in this solution. So it is also proved that the formation of MAO coating is a balance of the

growth and dissolution.

#### 4. Conclusion

We have demonstrated that an insulation layer with high impedance value is formed on the sample surface during the formation of the incipient film, which is a primary condition of the occurrence of arc striking phenomenon. The arc discharge of  $\text{OH}^-$  occurs followed by the formation of incipient film with high impedance value. Meanwhile, the dissolution process of ceramic coating is restrained by negatively charged ions such as  $\text{SiO}_3^{2-}$  and  $\text{CO}_3^{2-}$ . As an anodic oxide coating instead of the incipient film is prepared on the sample surface, it is helpful to advance the arc striking for the improving impedance value of the substrate.

#### Acknowledgements

This work was supported by the National Natural Science Foundation of China (No. 51201176), Ningbo Municipal Nature Science Foundation (No. 201101A6105005) and Director Foundation of Ningbo Institute of Materials Technology and Engineering (No. Y10317QF09).

#### REFERENCES

- [1] A.L. Yerokhin, X. Nie, A. Leyland, A. Matthews and S.J. Dowey: *Surf. Coat. Technol.*, 1999, **122**, 73.
- [2] H.F. Guo, M.Z. An, S. Xu and H.B. Huo: *Thin Solid Films*, 2005, **485**, 53.
- [3] Y. Yang and H. Wu: *J. Mater. Sci. Technol.*, 2010, **26**(10), 865.
- [4] A. Da Forno and M. Bestetti: *Surf. Coat. Technol.*, 2010, **205**, 1783.
- [5] M.H. Zhu, Z.B. Cai, X.Z. Lin, P.D. Ren, J. Tan and Z.R. Zhou: *Wear*, 2007, **263**, 472.
- [6] J.Z. Chen, Y.L. Shi, L. Wang, F.Y. Yan and F.Q. Zhang: *Mater. Lett.*, 2006, **60**, 2538.
- [7] H.F. Guo, M.Z. An, H.B. Huo, S. Xu and L.J. Wu: *Appl. Surf. Sci.*, 2006, **252**, 7911.
- [8] S.V. Genkov, O.A. Khrisanfova, A.G. Zavidnay, S.L. Sinebrukhov, A.N. Kovryanov, T.M. Scorobogatova and P.S. Gordienko: *Surf. Coat. Technol.*, 2000, **123**, 24.
- [9] X. Nie, A. Leyland and A. Matthews: *Surf. Coat. Technol.*, 2000, **125**, 407.
- [10] H.F. Guo and M.Z. An: *Thin Solid Films*, 2006, **500**(1–2), 186.
- [11] W.B. Xue, Z.W. Deng, R.Y. Chen and T.H. Zhang: *Thin Solid Films*, 2000, **372**, 114.
- [12] J.M. Li, H. Cai and B.L. Jiang: *Surf. Coat. Technol.*, 2007, **201**, 8702.
- [13] V.N. Malyshev and K.M. Zorin: *Appl. Surf. Sci.*, 2007, **254**, 1511.
- [14] K. Wu, Y.Q. Wang and M.Y. Zheng: *Mater. Sci. Eng. A*, 2007, **447**, 227.
- [15] Y.M. Wang, T.Q. Lei, B.L. Jiang and L.X. Guo: *Appl. Surf. Sci.*, 2004, **233**, 258.
- [16] J.M. Li, H. Cai, X.N. Xue and B.L. Jiang: *Mater. Lett.*, 2010, **64**: 2102.
- [17] Y. Han, J.F. Sun and X. Huang: *Electrochim. Acta*, 2008, **10**, 510.
- [18] P.I. Butyagin, Y.V. Khokhryakov and A.I. Mamaev: *Mater. Lett.*, 2003, **57**, 1748.